

Nb 가 Zr

Effects of Intermediate Annealing on the Corrosion Behavior of Niobium-containing Zirconium Alloys

150

Zr-0.4Nb-0.8Sn-FeCrMn Zr-1.5Nb-0.4Sn-Fe

Nb, 가 Nb 가 Nb 가 Nb 가 Zr(Fe,Cr)₂ 가 β- 가

가 β-Zr 가 β-Zr 가

Abstract

Effects of intermediate annealing temperature on the corrosion behavior were investigated for Zr-0.4Nb-0.8Sn-FeCrMn and Zr-1.5Nb-0.4Sn-Fe alloys that were intermediate annealed at various temperatures. The relationship between the corrosion behavior and the precipitation characteristics was discussed. The corrosion resistance of the alloys was apparently degraded with increasing intermediate annealing temperature, especially in Zr-1.5Nb-0.4Sn-Fe. Zr(Fe,Cr)₂-type precipitates were found in Zr-0.4Nb-0.8Sn-FeCrMn irrespective of intermediate annealing temperature. In Zr-1.5Nb-0.4Sn-Fe, β-Nb precipitated on lower-temperature annealing while β-Zr on higher-temperature annealing. The examination of particle size distribution revealed that the corrosion behavior of the alloys was dominantly affected by β-Zr larger than the specific size.

1.

Zircaloy-4 1990 가

Zircaloy-4 가 / pH

가 가 1 1960 Zircaloy-4 [1].

가 Zr 가 가 가 ,

[2-6]. , Nb 가 Zr 가 Zr

Nb 가 Zr

2.

Table 1
(1020) 200g button , 3 , Fig. 1 ,
15X20X1mm³ 가 800 가
5% HF, 45% HNO₃, 50% H₂O autoclave
360 water, 400 steam 360 70ppm LiOH 3가 210
TEM , 2 EDS . TEM
10% HClO₃, 90% C₂H₅OH twin-jet polishing .

3.

Fig. 2 A1 A2
가 가 가 가 가
Zr
3가
470°C

Fig. 3 A1 A2 static autoclave
360 360 70ppm LiOH 가 가 가
가 , 가 A 가 가
Nb 가 A2
가
가

Fig. 4 A1 A2 2

가 가 , , Nb 가
 A2
 A1 HCP Zr(Fe,Cr)₂
 β-Nb , A2 가 β-Zr 가 Fig.
 5, 6, 7 Zr(Fe,Cr)₂, β-Nb, β-Zr

Table 2

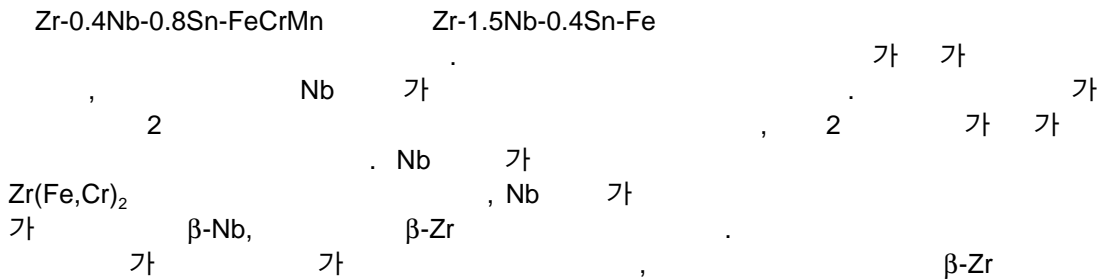
Nb 가 A1 Zr(Fe,Cr)₂
 , Nb 가 가 가 β-Nb, β-Zr
 , 가 A2 가 A1
 가 가 570°C (A) 가
 가 가 가 β-Zr
 2 가

Zircaloy-4 [4,6,7], Nb 가 가 가 가
 [8]. Nb 가 Zr 가 가
 Zr-Nb 2 [9,10] Nb 가
 β-Nb 2 가 가 50nm
 Zr-Nb-Sn 2 가 200nm
 가 80nm [11]. Zr-1Nb-1Sn-0.1Fe 2
 Fig. 8 [6]. 2

Nb 가 Zr 가 가
 Zircaloy , 1 [12].
 가 가 가

가 가 Nb 가 Zr
 2

4.



[1] F. Garzarolli, H. Stehle and E. Steinberg, Zirconium in the Nuclear Industry: Eleventh International Symposium, ASTM STP 1295, E. R. Bradley and G. P. Sabol, Eds., American Society for Testing and Materials, Philadelphia, 1996, pp. 12-32.

[2] G. P. Sabol, G. R. Kilp, M. G. Balfour and E. Roberts, Zirconium in the Nuclear Industry: Eighth International Symposium, ASTM STP 1023, L. E. P. Van Swam and C. M. Eucken, Eds., American Society for Testing and Materials, Philadelphia, 1989, pp. 227-244.

[3] A. V. Nikulina, A. M. Vladimir, M. M. Peregud, Y. K. Bibilashvili, V. A. Kotrehov, A. F. Lositsky, N. V. Kuzmenko, Y. P. Shevvin, V. K. Shamardin, G. P. Kobylansky and A. E. Novoselov, Zirconium in the Nuclear Industry: Eleventh International Symposium, ASTM STP 1295, E. R. Bradley and G. P. Sabol, Eds., American Society for Testing and Materials, Philadelphia, 1996, pp. 785-804.

[4] J. -P. Mardon, D. Charquet and J. Senevat, Zirconium in the Nuclear Industry: Twelfth International Symposium, ASTM STP 1354, G. P. Sabol and G. D. Moan, Eds., American Society for Testing and Materials, West Conshohocken, PA, 2000, pp. 505-524.

[5] K. Yamate, A. Oe, M. Hayashi, T. Okamoto, H. Anada and S. Hagi, Proceedings of the 1997 International Topical Meeting on LWR Fuel Performance, 1997, pp. 318-325.

[6] G. P. Sabol, R. J. Comstock, R. A. Weiner, P. Larouer and R. N. Stanutz, Zirconium in the Nuclear Industry: Tenth International Symposium, ASTM STP 1245, A. M. Garde and E. R. Bradley, Eds., American Society for Testing and Materials, Philadelphia, 1994, pp. 724-744.

[7] R. J. Comstock, G. Schoenberger and G. P. Sabol, Zirconium in the Nuclear Industry: Eleventh International Symposium, ASTM STP 1295, E. R. Bradley and G. P. Sabol, Eds., American Society for Testing and Materials, Philadelphia, 1996, pp. 710-725.

[8] H. Anada, K. Nomoto and Y. Shida, Zirconium in the Nuclear Industry: Tenth International Symposium, ASTM STP 1245, A. M. Garde and E. R. Bradley, Eds., American Society for Testing and Materials, Philadelphia, 1994, pp. 307-327.

[9] V. F. Urbanic, B. D. Warr, A. Manolescu, C. K. Chow and M. W. Shanahan, Zirconium in the Nuclear Industry: Eighth International Symposium, ASTM STP 1023, L. F. P. Van Swam and C. M. Eucken, Eds., American Society for Testing and Materials, West Conshohocken, PA, 1989, pp. 20-34.

[10] V. F. Urbanic and R. W. Gilbert, Proceedings of IAEA Technical Committee Meeting on Fundamental Aspects of Corrosion on Zirconium Base Alloys in Water Reactor Environments, International Atomic Energy Agency, Vienna, IWGFPT/34, 1990, pp. 262-272.

[11] G. P. Sabol, G. Schoenberger and M. G. Balfour, Proceedings of IAEA Technical Committee Meeting on Materials for Advanced Water Cooled Reactor, International Atomic Energy Agency, Vienna, IAEA-TECDOC-665, 1992, p. 122.

[12] H. Anada, B. J. Herb, K. Nomoto, S. Hagi, R. A. Graham and T. Kuroda, Zirconium in the Nuclear Industry: Eleventh International Symposium, ASTM STP 1295, E. R. Bradley and G. P. Sabol, Eds., American Society for Testing and Materials, Philadelphia, 1996, pp. 74-93.

Table 1. Chemical compositions of the Zr alloys used in this study (wt.%).

| | Nb | Sn | Fe | Cr | Mn | Zr |
|----|-----|-----|-----|-----|-----|---------|
| A1 | 0.4 | 0.8 | 0.3 | 0.2 | 0.1 | Balance |
| A2 | 1.5 | 0.4 | 0.1 | | | Balance |

Table 2. Characteristics of precipitates in the Zr alloys manufactured by different annealing conditions.

| | Process A | | Process B | | Process C | |
|----|--|-------------------------------|--|-------------------------------|--|-------------------------------|
| A1 | Zr(Fe,Cr) ₂ HCP 52 nm | | Zr(Fe,Cr) ₂ HCP 69 nm | | Zr(Fe,Cr) ₂ HCP 85 nm | |
| A2 | β -Nb BCC | Zr(Fe,Cr) ₂ HCP | β -Zr BCC | Zr(Fe,Cr) ₂ HCP | β -Zr BCC | Zr(Fe,Cr) ₂ HCP |
| | 53 nm | | 73 nm | | 178 nm | |

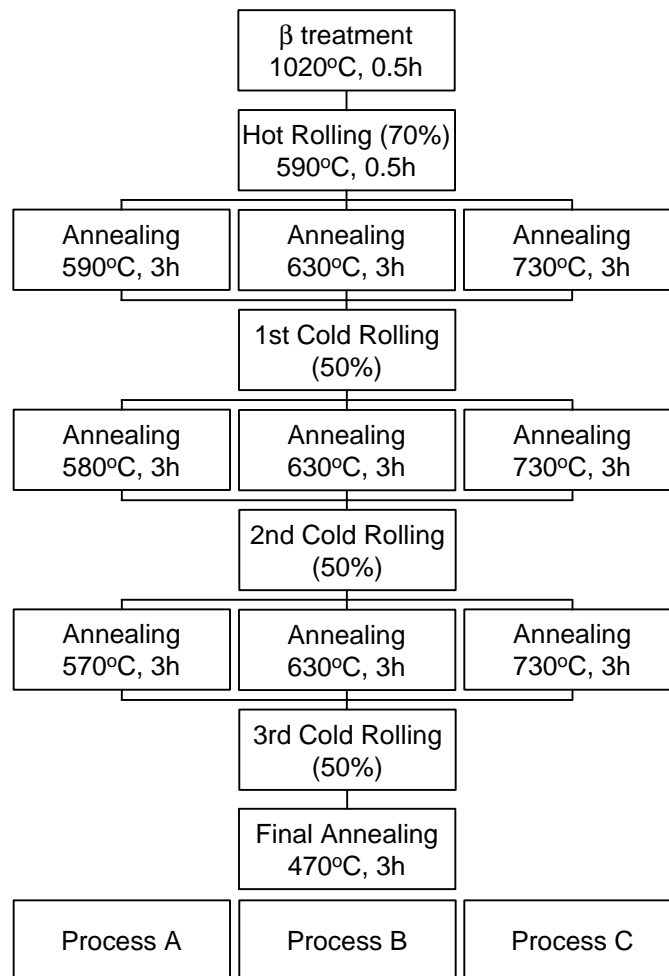


Fig. 1. Flow chart of manufacturing process for sheet specimens.

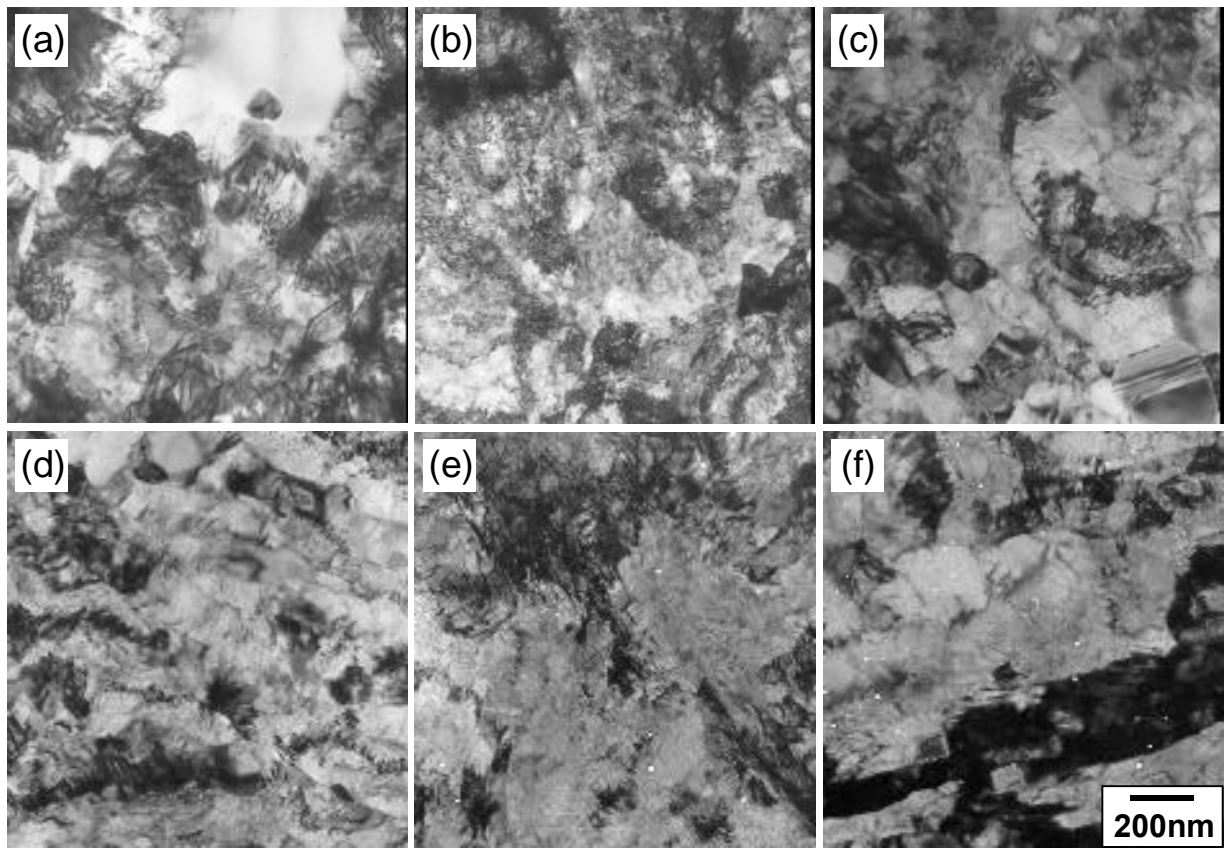


Fig. 2. Transmission electron micrographs of (a, b, c) Zr-0.4Nb-0.8Sn-FeCrMn and (d, e, f) Zr-1.5Nb-0.4Sn-Fe alloys after stress-relieving at 470°C for 3h.

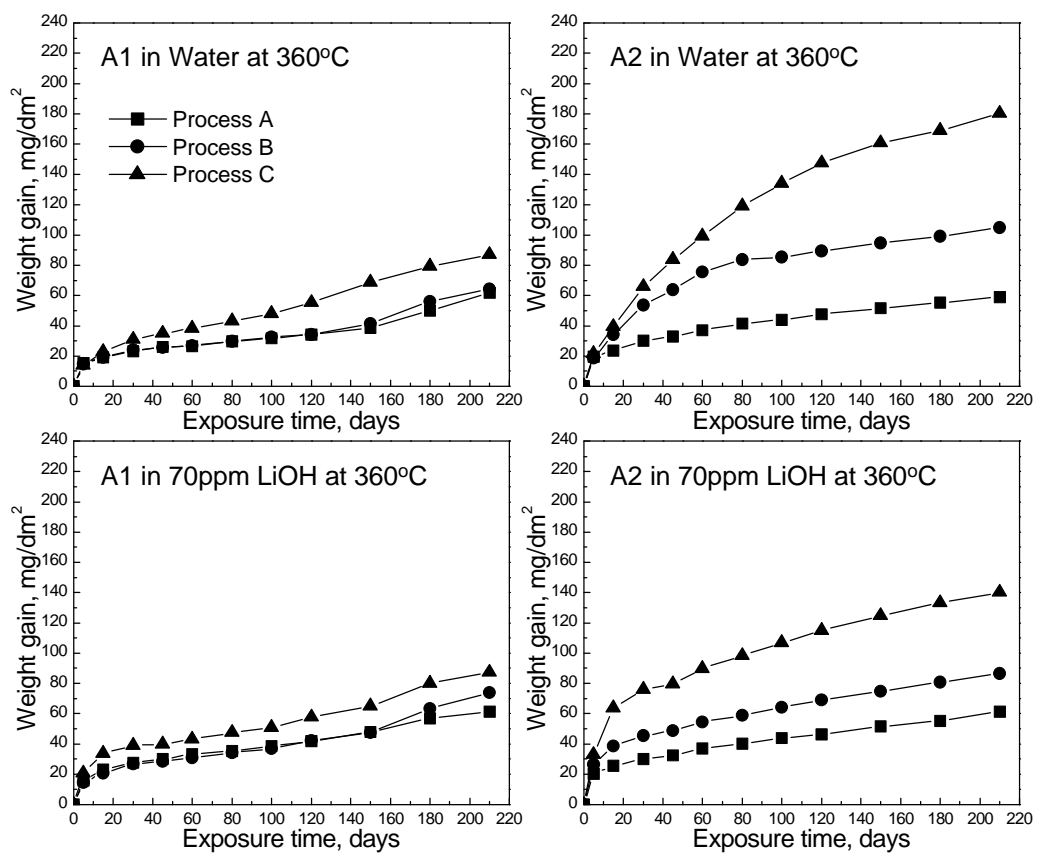


Fig. 3. Corrosion behavior of Zr-0.4Nb-0.8Sn-FeCrMn (A1) and Zr-1.5Nb-0.4Sn-Fe (A2) alloys at 360°C in pure water and in lithiated water containing 70ppm Li.

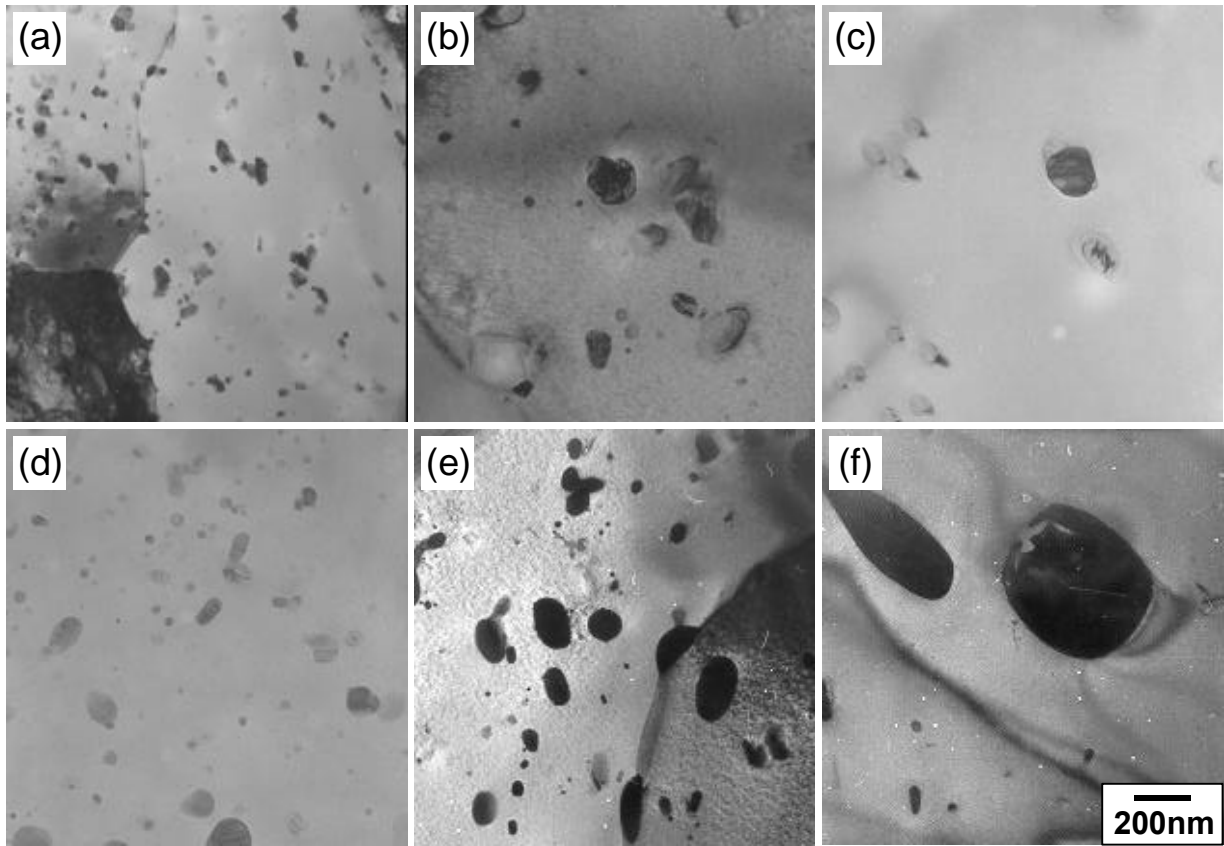


Fig. 4. Transmission electron micrographs of precipitates in (a, b, c) Zr-0.4Nb-0.8Sn-FeCrMn and (d, e, f) Zr-1.5Nb-0.4Sn-Fe alloys that were intermediate-annealed at (a, d) 570°C, (b, e) 630°C and (c, f) 730°C.

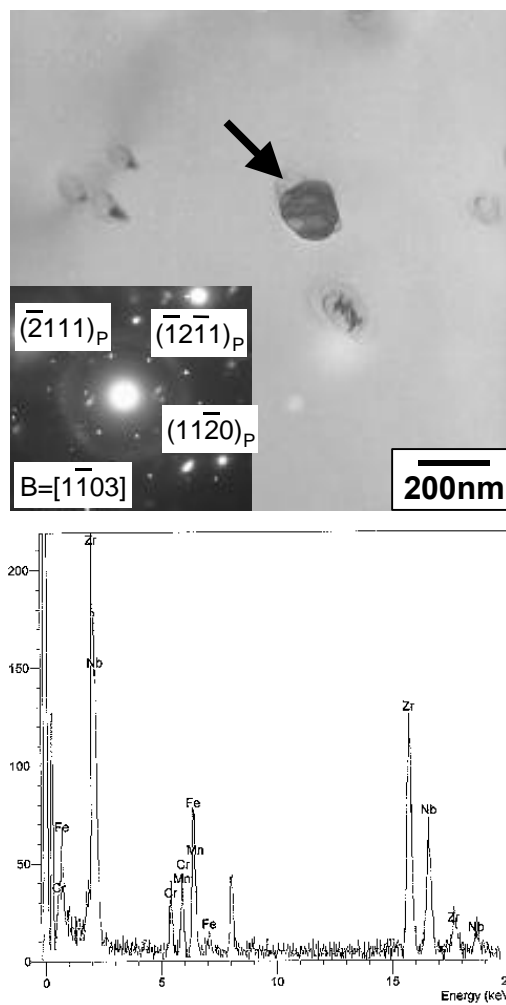


Fig. 5. TEM bright field image, selected area diffraction pattern and EDS spectrum of $Zr(Fe,Cr)_2$ -type precipitate in $Zr-0.4Nb-0.8Sn-FeCrMn$ alloys that were intermediate-annealed at 730°C for 3h.

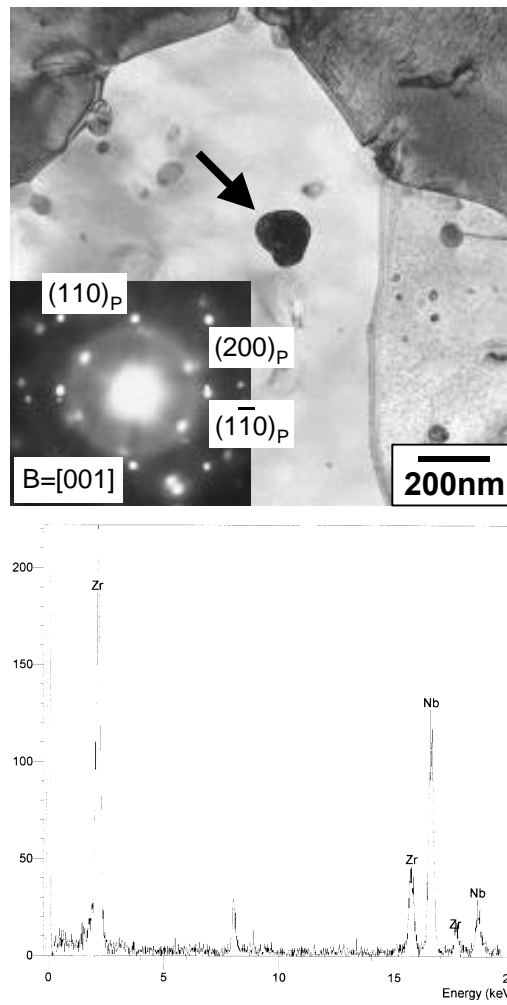


Fig. 6. TEM bright field image, selected area diffraction pattern and EDS spectrum of β -Nb precipitate in Zr-1.5Nb-0.4Sn-Fe alloys that were intermediate-annealed at 570°C for 3h.

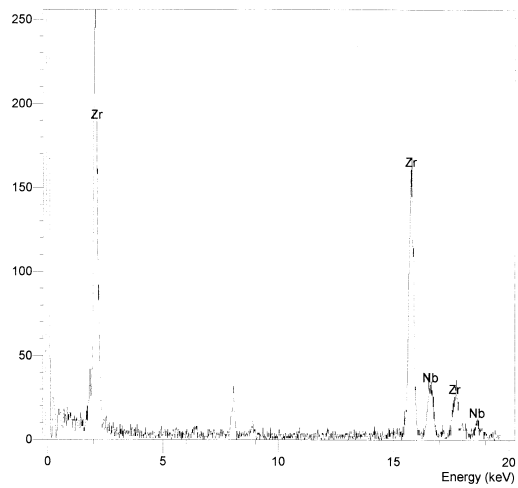
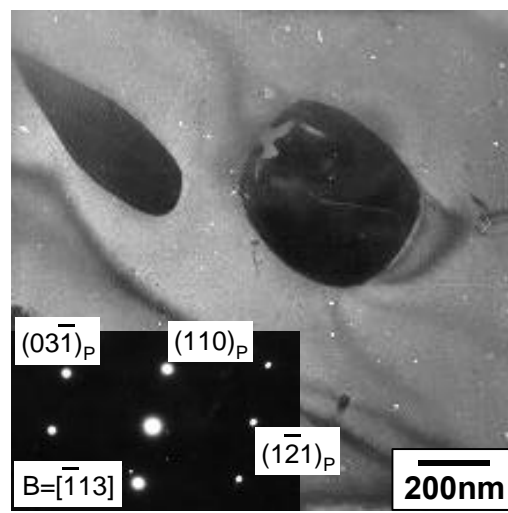


Fig. 7. TEM bright field image, selected area diffraction pattern and EDS spectrum of β -Zr precipitate in Zr-1.5Nb-0.4Sn-Fe alloys that were intermediate-annealed at 730°C for 3h.

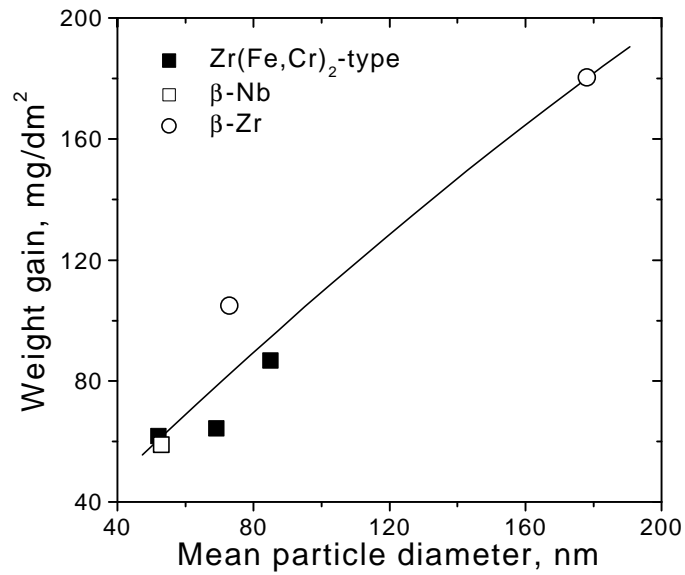


Fig. 8. Relationship between mean particle diameter and weight gain, showing that mean particle size is well correlated with corrosion resistance of the alloys irrespective of precipitate types.